METEORITICAL PERSPECTIVE ON THE ORIGIN OF R-PROCESS NUCLIDES IN THE SOLAR SYSTEM. T. Yokoyama[1], R. Fukai[1], and T. Tsujimoto[2] [1]Department of Earth and Planetary Sciences, Tokyo Institute of Technology, Japan. [2]National Astronomical Observatory of Japan, (tetsuya.yoko@geo.titech.ac.jp).

Introduction: Isotopes of elements heavier than Fe are mainly produced by stellar nucleosyntheses of the *s*-, *r*-, and *p*-processes. Compared to the *s*-process, the mechanism and stellar environment for the *r*-process are still unclear. Although neutrino-driven wind from a nascent neutron star of core-collapse supernova (ccSN) is known to be the major source of *r*-process nuclides, electron fraction per nucleon is too high to produce heavy *r*-nuclides of mass number (A) beyond 130 [1]. In contrast, several lines of evidence affirm the production of abundant heavy *r*-nuclides with A > 130 by the merger of two neutron stars (NSM) in a binary system [2]. Furthermore, ccSNe induced by strong magnetic fields and/or fast rotation of the stellar core (MR-SNe) are considered to be an alternative *r*-process site [3].

Direct isotopic analysis of presolar grains has been the major meteoritical approach for the study of stellar nucleosynthesis, yet isotopic data for trans-Fe elements in single presolar grains are scarcely obtained with some exceptions [e.g., 4]. Alternatively, detection of subtle isotope anomalies in bulk meteorites for trans-Fe elements (e.g., Sr, Zr, Mo, Ru) offers another opportunity to understand the origin of *r*-nuclides in the Solar System [5-6]. In particular, bulk carbonaceous chondrites and some iron meteorites (CC-group) are found to have *r*-process excesses compared to the other meteorites (NC-group) [7-9], suggesting the presence of two isotopically distinct reservoirs in the solar nebula [10]. The mechanism that generated the observed *r*-process excesses in the CC-group is not fully understood yet; the proposed model includes heterogeneous injection of grains from a nearby SN [11], physical sorting of isotopically anomalous grains [12], and selective destruction of thermally weak presolar grains [13].

In this study, we compiled literature data and analyzed the isotopic compositions of trans-Fe elements in bulk meteorites with a specific emphasis on the anomalies of *r*-process nuclides as a function of isotopic mass and the 50% condensation temperature ($T_{50\%}$) of each element. Additionally, we determined the Yb isotopic compositions in some chondrites. Yb is a heavy lanthanide that has seven stable isotopes with different contributions from the *s*-, *r*-, and *p*-processes, of which the *r*-nuclides (A = 171–176) are too heavy to be produced by ccSNe. The $T_{50\%}$ for Yb (1487 K) is lower than those of the neighboring lanthanides (1659 K) and is comparable to that of Sr (1464 K) [14]. These unique characteristics of Yb make it possible to place an additional constraint on the mechanism that gave rise to *r*-process excesses in the CC-group meteorites, which further provides vital information regarding the origin of *r*-process nuclides in the Solar System.

Yb isotope analysis: We analyzed Yb isotopes of four chondrites (Murchison, CM2; Olivenza, LL5; Saint-Séverin, LL6; NWA 753, R3.9) and two terrestrial basalts (JB-2a, JB-3). Murchison was digested at high PT condition using HF, HNO_3, and H_2SO_4 to completely dissolve presolar grains [15]. The rest of the samples were decomposed by HF, HNO_3, and $HClO_4$. Yb was separated by passing through a cation exchange resin and an extraction chromatographic resin (LN resin, Eichrom). Yb isotopes were measured using TIMS by the dynamic multicollection and multistatic methods [16].

Data Compilation: In addition to the newly obtained Yb isotope data, we compiled high precision isotopic compositions of 11 elements (Sr, Zr, Mo, Ru, Te, Ba, Nd, Sm, Hf, W, and Os) in bulk aliquots of CC- and NC-group meteorites [e.g., 7-9, 16-27]. For simplification, we ignored the isotopes that are free from the *r*-process (e.g., pure *p*-nuclides). To quantitatively analyze the extent of *r*-process excesses in individual meteorites, we determined the *r*-process enrichment factor (η_r) for an isotope ratio R (= i/j) as defined by the following equation;

$$\eta_r = \frac{R_s - R_m/[j]_t}{R_t - R_m/[j]_s} \cdot 10^6 \qquad (1)$$

where [j] is the number of atom for the isotope j, and subscripts m, t, and s represent meteorite, terrestrial, and *s*-process end-component [28], respectively.

Results: The Yb isotope ratios for terrestrial and meteorite samples are reported as μYb notations that represent the parts par 10^6 deviations from the standard (Alfa Aesar Yb). As presented in Fig. 1, we observed no Yb anomalies in terrestrial and meteorite samples that exceeded the range of analytical uncertainties.

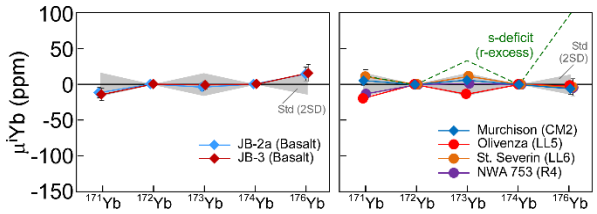

Fig. 1 μYb values of terrestrial rocks and chondrites.

Fig. 2 shows the η_r values of CC- and NC-group meteorites for the 12 trans-Fe elements. The η_r values of

CC-meteorites are prominent for Sr, Zr, and Mo, while the values decrease toward Te. Except for Ba and Nd, elements beyond Te do not show anomalies in *r*-process isotopes. For NC-meteorites, small excesses can be seen for Zr, Mo, and Ru, whereas the other elements do not show such excesses.

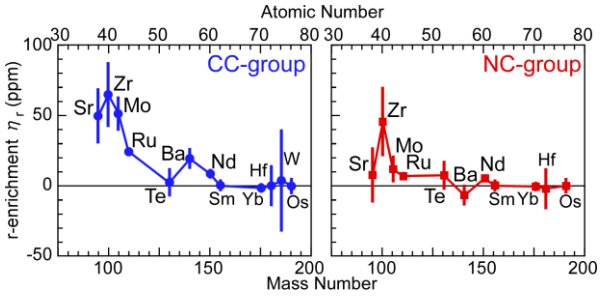

Fig. 2 η_r values of CC- and NC-group meteorites.

Discussion: The η_r values of individual elements for CC-meteorites are displayed as a function of $T_{50\%}$ and atomic number (Fig. 3). As can be seen in this figure, the extent of *r*-excess in CC-meteorites is controlled mainly by the mass of nuclides rather than the $T_{50\%}$ of individual elements. The dependency of mass number is also evident when the pattern of η_r for CC meteorites (Fig. 2, left) and the *r*-process production rate for a normal ccSN (Fig. 4, left) are compared. These results indicate that the grains ejected from normal ccSNe would be responsible for the *r*-excesses in CC-meteorites for light elements from Sr to Ru. Dust grains carrying heavy *r*-nuclides were not involved in the processes that caused *r*-excesses for light elements in CC-meteorites. On the other hand, an additional process is needed to explain the isotope anomalies for Ba and Nd, possibly relevant to the behavior of *s*-process carriers.

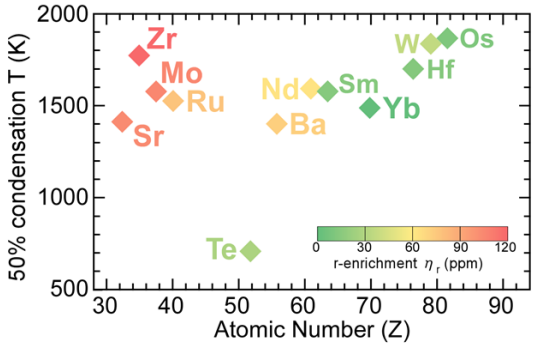

Fig. 3 η_r values of CC meteorites displayed in a color chart as a function of $T_{50\%}$ and atomic number.

From the discussion above, we place a constraint on the origin of *r*-process nuclides in the Solar System. The *r*-nuclides in the Solar System are the integration of multiple nucleosynthetic processes occurred in the Galaxy including the normal ccSNe, MR-SNe, and NSM. Importantly, the lifetime of dust grains in the Galaxy is estimated to be up to 10^7 years [29]. Therefore, the carrier phases of *r*-nuclides produced more than 10^7 years before the start of the Solar System must have been all destroyed and *r*-nuclides were homogeneously distributed in the molecular cloud. On the other hand, the pattern of η_r for CC meteorites (Fig. 2) suggests that fresh *r*-nuclides synthesized within 10^7 years before the onset of the Solar System must be dominantly originated from the normal ccSNe. We conclude that dust grains from such ccSNe, containing only light elements, were heterogeneously distributed in the solar nebula at the time of planetesimal formation.

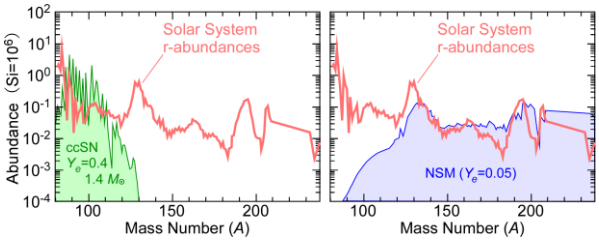

Fig. 4 R-process production rates for a normal ccSN (left: ref. [1]) and neutron star mergers (right: ref. [30]). Solar r-process abundances are obtained from ref. [31].

References: [1] Wanajo S. (2013) *ApJ, 770,* L22. [2] Thielemann, F.K. et al. (2017) *Annu. Rev. Nucl. Part. Sci. 67,* 253. [3] Nishimura N. et al. (2015) *ApJ, 810,* 109. [4] Nicolussi G.K. et al. (1997) *Science, 277,* 1281. [5] Yokoyama T. and Walker R.J. (2016) *RiMG, 81,* 107. [6] Dauphas N. and Schauble E.A. (2016) *Annu. Rev. Earth Planet. Sci., 44,* 709. [7] Budde G. et al. (2016) *EPSL, 454,* 293. [8] Worsham E.A. et al. (2017) *EPSL, 467,* 157. [9] Kruijer T.S. et al. (2017) *PNAS, 114,* 6712. [10] Warren P.H. (2011) *EPSL, 311,* 93. [11] Qin L. et al. (2011) *GCA, 75,* 629. [12] Dauphas N. et al. (2011) *ApJ, 720,* 1577. [13] Trinquier A. et al. (2009) *Science, 324,* 374. [14] Lodders K. (2003) *ApJ, 591,* 1220. [15] Yokoyama T. et al. (2015) *EPSL, 416,* 46. [16] Yokoyama T. et al. (2016) *LPS XLVII,* Abstract #2418. [17] Moynier F. et al. (2012) *ApJ, 758,* 45. [18] Akram W. et al. (2015) *GCA, 165,* 484. [19] Burkhardt C. et al. (2011) *EPSL, 312,* 390. [20] Fischer-Gödde M. et al. (2015) *GCA, 168,* 151. [21] Fehr M.A. et al. (2006) *GCA, 70,* 3436. [22] Bermingham K.R. et al. (2016) *GCA, 175,* 282. [23] Burkhardt C. et al. (2016) *Nature, 537,* 394. [24] Fukai R. and Yokoyama, T. (2017) *EPSL, 474,* 206. [25] Akram W. et al. (2013) *ApJ, 777,* 169. [26] Kleine T. et al. (2004) *GCA, 68,* 2935. [27] Yokoyama T. et al. (2010) *EPSL, 291,* 48. [28] Arlandini C. et al. (1999) *ApJ, 525,* 886. [29] Bekki K. (2015) *MNRAS, 449,* 1625. [30] Wanajo S. (2014) *ApJL, 789,* L39. [31] Käppeler F. et al. (1989) *Rep. Prog. Phys., 52,* 945.